

ORIGINAL ARTICLE

OPEN

Effects of intestine-specific deletion of FGF15 on the development of fatty liver disease with vertical sleeve gastrectomy

Monica D. Chow¹ | Katherine Otersen²  | Andrew Wassef^{3,4,5,6} | Bo Kong²  | Sowmya Yamarthy²  | Daniel Rizzolo²  | Ill Yang⁷  | Brian Buckley⁷  | Alexander Lu²  | Naomi Crook² | Matthew Lee² | Judy Gao² | Sareena Naganand² | Mary F. Stofan²  | Laura Armstrong²  | Justin Schumacher²  | Rulaiha Taylor²  | Zakiyah Henry²  | Veronia Basaly²  | Zhenning Yang²  | Min Zhang⁸  | Mingxing Huang⁹  | Leonid Kagan^{3,4} | Luigi Brunetti^{3,4}  | Ragui Sadek^{5,6} | Yi-Horng Lee¹  | Grace L. Guo^{2,7,10,11} 

¹Department of Surgery, Division of Pediatric Surgery, Rutgers Robert Wood Johnson Medical Center School, New Brunswick, New Jersey, USA

²Department of Pharmacology and Toxicology, Rutgers University, Piscataway, New Jersey, USA

³Department of Pharmaceutics, Ernest Mario School of Pharmacy-Rutgers University, Piscataway, New Jersey, USA

⁴Center of Excellence for Pharmaceutical Translational Research and Education, Rutgers University, Piscataway, New Jersey, USA

⁵Center of Excellence for Metabolic and Bariatric Surgery, Robert Wood Johnson Barnabas University Hospital, New Brunswick, New Jersey, USA

⁶Advanced Surgical & Bariatrics of NJ, Somerset, New Jersey, USA

⁷Environmental and Occupational Health Science Institute, Rutgers University, Piscataway, New Jersey, USA

⁸Children's Liver Disease Center, 302 Military Hospital, Beijing, China

⁹Department of Infectious Diseases, the Fifth Affiliated Hospital of Sun Yat-Sen University (SYSU), Zhuhai, Guangdong, China

¹⁰Department of Veterans Affairs New Jersey Health Care System, East Orange, New Jersey, USA

¹¹Rutgers Center for Lipid Research, New Brunswick, New Jersey, USA

Correspondence

Grace L. Guo, Department of Pharmacology and Toxicology, Ernest Mario School of Pharmacy, Rutgers University, 170 Frelinghuysen Road, Piscataway, NJ 08854, USA.
 Email: guo@eohsi.rutgers.edu

Abstract

Background: Vertical sleeve gastrectomy (SGx) is a type of bariatric surgery to treat morbid obesity and metabolic dysfunction-associated steatotic liver disease (MASLD). The molecular mechanisms of SGx to improve MASLD are unclear, but increased bile acids (BAs) and FGF19

Monica D. Chow, Katherine Otersen, Andrew Wassef, and Bo Kong contributed equally.

Abbreviations: ALT, alanine aminotransferase; Asbt, apical sodium-dependent bile acid transporter; AST, aspartate transaminase; BA, bile acid; BMI, body mass index; BW, body weight; CHTN, Cooperative Human Tissue Network; DCA, deoxycholic acid; FXR, farnesoid X receptor; GLP1, glucagon-like peptide 1; HFD, high-fat diet; Ibbp, ileal bile acid-binding protein; MASH, metabolic dysfunction-associated steatohepatitis; MASLD, metabolic dysfunction-associated steatotic liver disease; NDRI, National Disease Research Interchange; Ostβ, organic solute transporter beta; SGx, vertical sleeve gastrectomy; TCA, taurine-conjugated cholic acid; TGR5, G-protein-coupled bile acid receptor, GPBAR1; WT, wild type.

Supplemental Digital Content is available for this article. Direct URL citations are provided in the HTML and PDF versions of this article on the journal's website, www.hepcommjournal.com.

This is an open access article distributed under the terms of the Creative Commons Attribution-Non Commercial-No Derivatives License 4.0 (CCBY-NC-ND), where it is permissible to download and share the work provided it is properly cited. The work cannot be changed in any way or used commercially without permission from the journal.

Copyright © 2024 The Author(s). Published by Wolters Kluwer Health, Inc. on behalf of the American Association for the Study of Liver Diseases.

(mouse FGF15) were observed. FGF15/19 is expressed in the ileum in response to BAs and is critical in not only suppressing BA synthesis in the liver but also promoting energy expenditure. We hypothesized the reduction of obesity and resolution of MASLD by SGx may be mediated by FGF15/19.

Methods: First, we conducted hepatic gene expression analysis in obese patients undergoing SGx, with the results showing increased expression of FGF19 in obese patients' livers. Next, we used wild-type and intestine-specific *Fgf15* knockout mice (*Fgf15*^{ile-/-}) to determine the effects of FGF15 deficiency on improving the metabolic effects.

Results: SGx improved metabolic endpoints in both genotypes, evidenced by decreased obesity, improved glucose tolerance, and reduced MASLD progression. However, *Fgf15*^{ile-/-} mice showed better improvement compared to wild-type mice after SGx, suggesting that other mediators than FGF15 are also responsible for the beneficial effects of FGF15 deficiency. Further gene expression analysis in brown adipose tissue suggests increased thermogenesis.

Conclusions: FGF15 deficiency, the larger BA pool and higher levels of secondary BAs may increase energy expenditure in extrahepatic tissues, which may be responsible for improved metabolic functions following SGx.

INTRODUCTION

Obesity is an increasing public health concern as worldwide prevalence has approximately tripled over the last half century. Obesity is highly associated with metabolic syndrome and a variety of comorbidities, including metabolic dysfunction–associated steatotic liver disease (MASLD). MASLD represents a spectrum of liver pathologies, ranging from simple steatosis, metabolic dysfunction–associated steatohepatitis (MASH), to fibrosis. Left unattended, MASH-induced fibrosis may progress to cirrhosis or even HCC. Currently, there is no FDA-approved therapy for MASH and the only recommendation is lifestyle modification.^[1] If lifestyle modification and diet fail to combat obesity, only surgical options are left for patients, including adjustable gastric bands, Roux-en-Y-gastric bypass, biliopancreatic division with a duodenal switch, or vertical sleeve gastrectomy (SGx).^[2]

SGx represents the most routinely performed bariatric surgery.^[2] Following SGx, insulin secretion and sensitivity improve immediately even before substantial weight loss,^[3] suggesting that changes to insulin resistance occur independently from weight loss and the changes may be linked to hormonal alterations immediately after surgical intervention. Indeed, following SGx, there are changes in a variety of endocrine factors and metabolites associated with beneficial effects including insulin sensitivity and weight loss.

Among these, an increase in the levels of total bile acids (BAs) has been reported in several human and animal studies.^[4–6] BAs are amphipathic molecules and activate several nuclear and membrane receptors, with increasing evidence showing the critical roles of BAs in the regulation of lipid and energy homeostasis.^[7–10] BAs are endogenous ligands of a nuclear receptor, farnesoid X receptor (FXR).^[11] Although the roles of FXR in mediating the beneficial effects of bariatric surgeries are unclear, there are emerging studies that initiate mechanistic approaches in deciphering the underlying molecular pathways. It was first reported that FXR is required for the beneficial effects of SGx as whole-body deletion of FXR in mice diminished these beneficial effects.^[12] In agreement, hepatic transcriptome profile in patients undergoing bariatric surgery showed induction of an alternative BA synthesis pathway that synthesizes the most potent endogenous FXR ligand.^[8] FXR is expressed in multiple cells and there is an increasing understanding of tissue-specific effects of FXR in regulating BA homeostasis, liver and gut functions, and energy metabolism.^[13,14] While intestinal FXR is emerging to be the most important regulator for BA synthesis in the liver,^[14,15] both hepatic and intestinal FXR are critical in regulating pathways involved in energy metabolism. One of the most strongly induced target genes of FXR in the intestine, specifically the ileum, is FGF15 (*Fgf15*) in mice and *FGF19* in humans. In addition to potentially suppressing BA synthesis in the

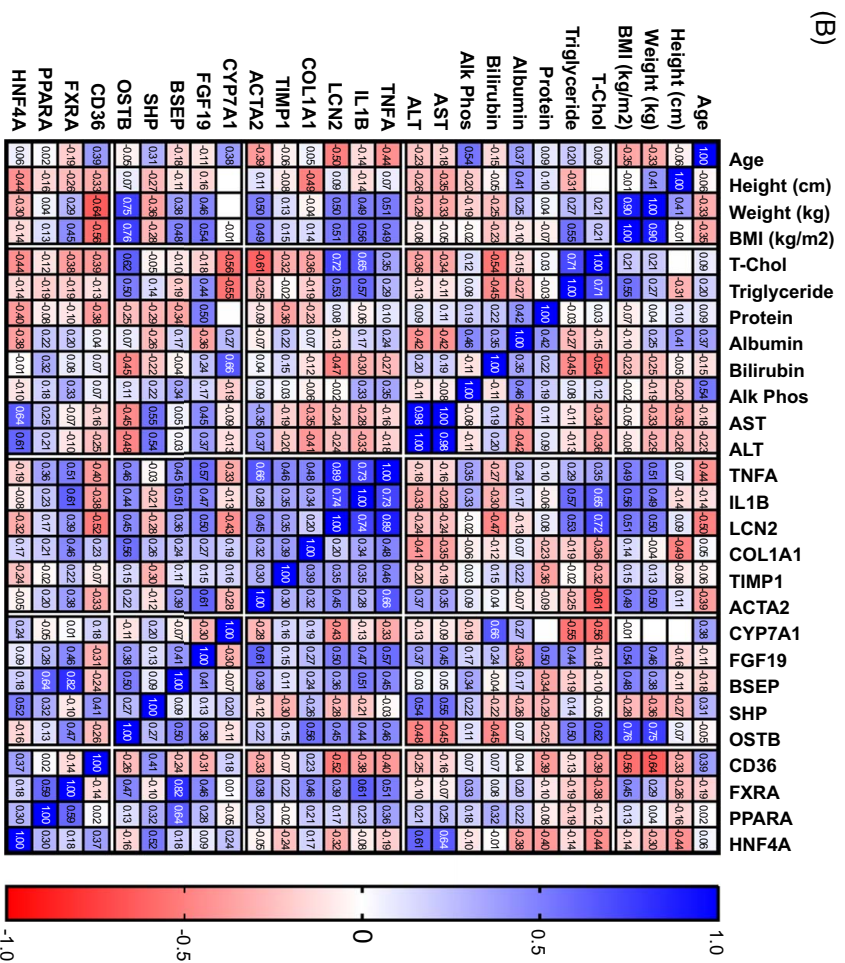
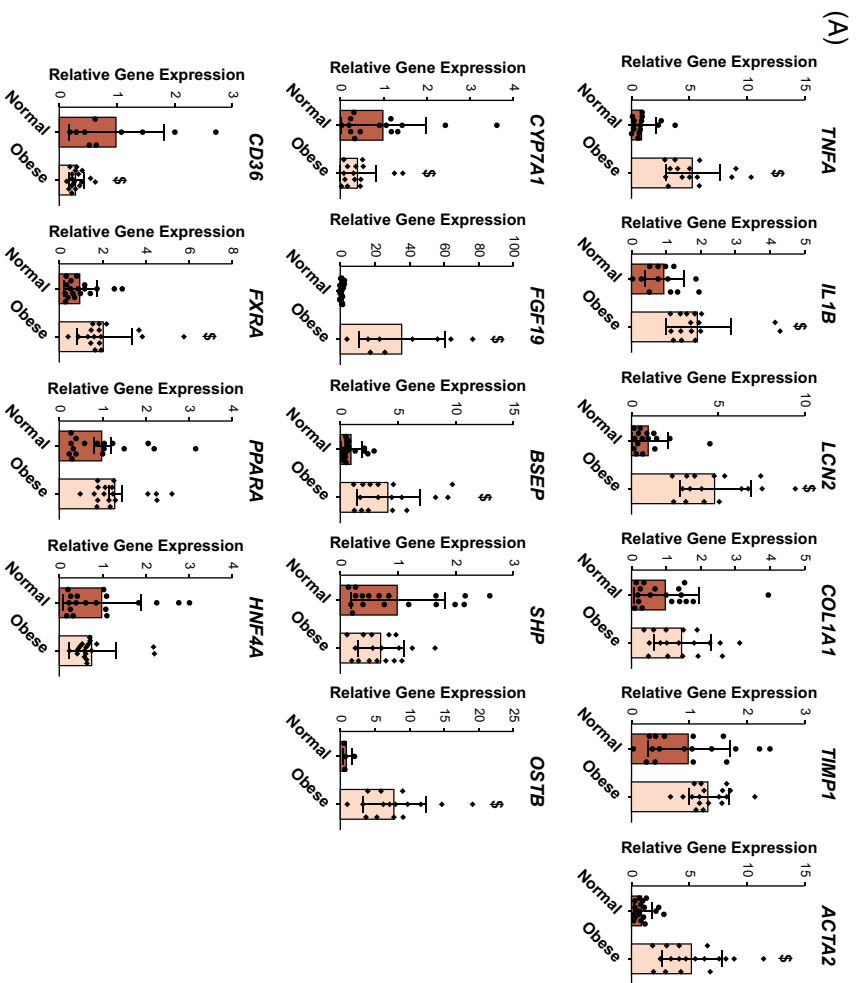


FIGURE 1 Relative gene expression in livers of control versus obese patients. The human samples are described in the Methods section. (A) The hepatic expression of genes involved in BA metabolism, lipid homeostasis, inflammation, and fibrosis was determined by real-time qPCR. (B) Association among the patients' clinical parameters and hepatic expression of genes listed in (A). \$ indicates statistical significance ($p < 0.05$). Abbreviations: BA, bile acid; BMI, body mass index.

liver,^[14,16] FGF15/19 acts very effectively in increasing energy expenditure and reducing body weight.^[17,18] Furthermore, BAs participate in the regulation of energy homeostasis in an FXR/FGF15/19-independent manner. Specifically, the secondary BAs, including deoxycholic acid (DCA) and lithocholic acid, have been shown to activate a membrane receptor, G-protein-coupled bile acid receptor, GPBAR1 (TGR5).^[19] GPBAR1 is highly expressed in the L cells in the terminal ileum and brown adipocytes, and once this receptor is activated, it leads to the induction of glucagon-like peptide 1 (GLP1) and other genes involved in thermogenesis.^[20,21]

Several studies have been conducted to determine the role of FGF15 in regulating energy homeostasis.^[5,22] A recent human study reported an increase in FGF19 levels following bypass surgery.^[8] However, the role of FGF15 in mediating the beneficial effects of SGx is unclear, and it is unknown to what extent FGF15 is involved in reducing MASLD development following SGx. Therefore, it is crucial to determine whether FGF15 plays a role in mediating the beneficial effects of SGx. In this study, we determined the effects of FGF15 deficiency in mediating the beneficial effects of SGx, using enterocyte-specific FGF15 knockout mice (*Fgf15^{ile-/-}*).

METHODS

Patients' enrollment

This prospective noninterventional study recruited (N=30, body mass index ≥ 35) patients, aged 18–80 years, undergoing bariatric surgery, requiring laparoscopic liver biopsy for suspected chronic liver disease. Liver biopsies, obtained through wedge or needle core technique from the left liver lobe, were divided. A portion underwent standard pathological diagnosis, while the rest was allocated for research. Collected biopsies were promptly placed on ice, transported, and flash-frozen within 15 minutes to preserve the cellular and molecular integrity of the specimen.

Control liver specimens (N=30, body mass index ≤ 30) were sourced from established channels: the Cooperative Human Tissue Network (CHTN) and the National Disease Research Interchange (NDRI). Links to their respective websites: <https://www.chtn.org/about/index.html> and <https://ndriresource.org/about-us>. CHTN, backed by the National Cancer Institute, furnishes human biospecimens and fluids from routine

medical procedures for research purposes. NDRI, a nonprofit, provides human tissues from diverse healthy and afflicted donors. A standardized data set, encompassing demographic details (age, race, and gender), alongside tissue diagnosis quality control, was obtained from CHTN and NDRI. Accompanying the samples were deidentified pathology reports, following established confidentiality norms. The use of these deidentified human specimens was determined as exempt research by the Rutgers Biomedical Health Sciences Institutional Review Board (Pro2019001020).

A total of (N=60) subjects were included. After exclusions, the study retained (N=30) participants. Exclusions were made for specimens from subjects with infectious diseases, a history of alcohol abuse/addiction, hepatitis A, B, or C infection (self-reported/medical records), and poor RNA quality. Ethical compliance was ensured through approval from the RBHS institutional review board under protocols Pro2020002744 and Pro2019001020, safeguarding ethical guidelines and participant welfare.

Animals and treatment

Fgf15^{ile-/-} were developed through breeding *Fgf15^{ile+/+}* floxed/floxed and villin Cre+ mice.^[23] All animals were group-housed in a temperature-controlled and pathogen-free facility with a 12-hour light/dark cycle and given food and water ad libitum.

Fgf15^{ile-/-} (*Fgf15* floxed/floxed and cre+) and *Fgf15^{ile+/+}* (wild type, WT; *Fgf15* floxed/floxed and cre-) were fed a high-fat diet (HFD; 60% calories from lard, 20% calories from carbohydrate, containing 0.2796% cholesterol, Research Diets catalog #D12492, New Brunswick, NJ) for 3 months to induce obesity. Following 3-month HFD feeding, the mice underwent either a sham operation (Sham) or SGx. Briefly, SGx surgery was performed using an aseptic surgical technique. Approximately 80% of the stomach along the greater curvature was resected, and the remaining stomach was closed with a running suture. The stomach was introduced back into the abdominal cavity.

The mice were kept on a 10-day liquid diet (Ensure Vanilla Protein Shake) immediately postoperatively, after which the HFD was reintroduced. Mice were necropsied at 1-, 2- or 3-months postoperatively in the morning without fasting, and blood, liver, ileum, and brown adipose tissues were collected after euthanasia (Figure 2A). Only male mice were used in this study due to the higher sensitivity to diet-induced obesity in male

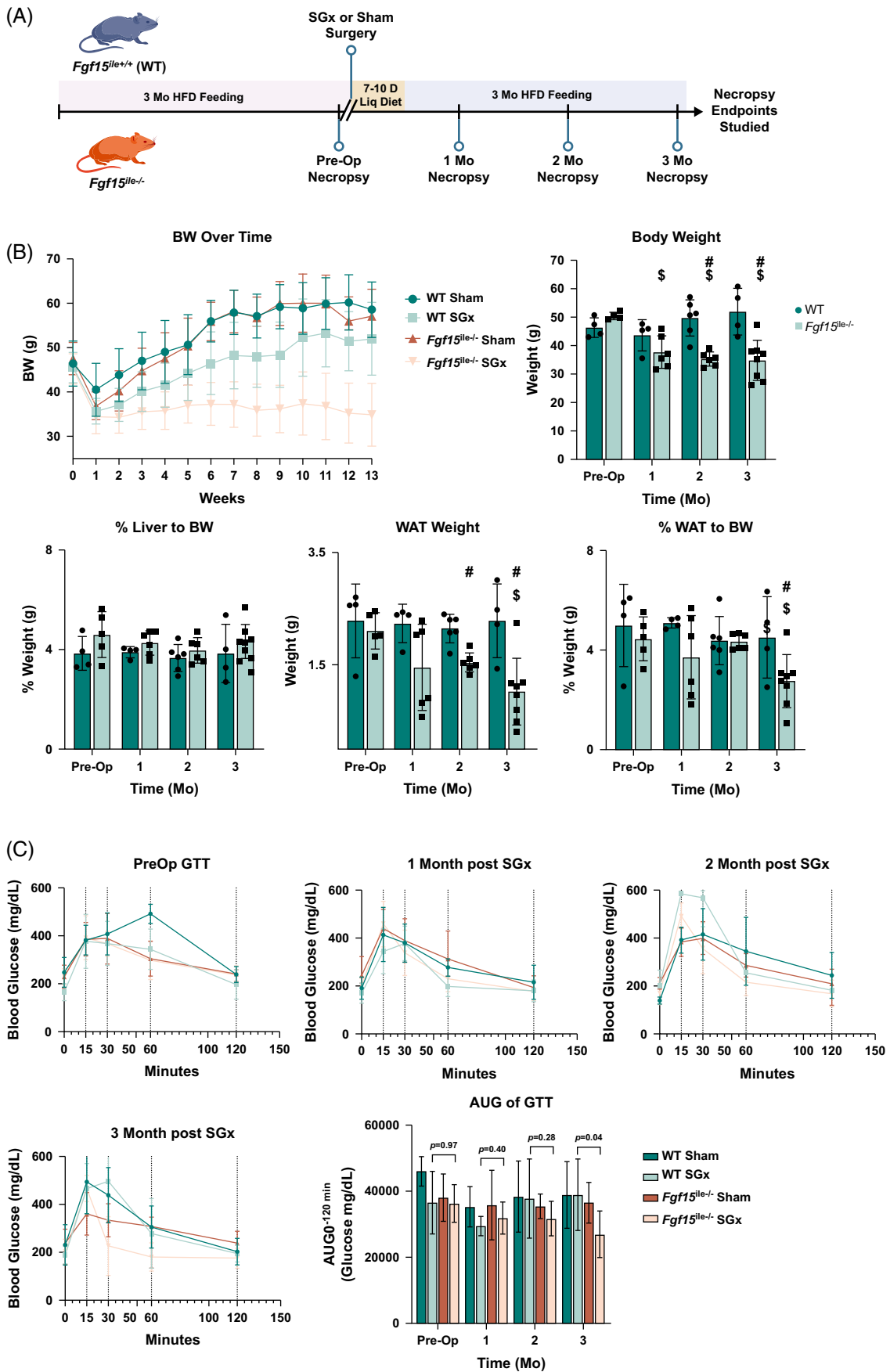


FIGURE 2 Intestine-specific deletion of *Fgf15* altered response to SGx. (A) Experimental design and timeline of mouse treatment. (B) BW change after surgery over time; BW and WAT weight along with % LW and %WAT in both WT and *Fgf15*^{le-/-} mice observed preop, 1, 2, and 3 months postop (WT: n = 4, 4, 6, 4, respectively; *Fgf15*^{le-/-}: n = 5, 6, 6, 8, respectively). (C) Glucose tolerance test after HFD-feeding compared to preop and sham surgery. Blood glucose levels in Sham and SGx following 3 months of postoperative feeding at 4 time points: preop, 1, 2, and 3 months with measurements taken at 0-, 15-, 30-, 60-, and 120-minute intervals for the 3-month group. AUC at 3 months feeding for Sham and SGx in both genotypes. \$ is for statistical significance ($p < 0.05$) within the same genotype compared to preop control. # is for statistical significance ($p < 0.05$) within the same time point between WT and *Fgf15*^{le-/-} mice. Abbreviations: BW, body weight; HFD, high-fat diet; LW, liver weight; SGx, vertical sleeve gastrectomy; WAT, white adipose tissue.

mice. All animal experiments were approved by the Institutional Animal Care and Use Committee (IACUC) at Rutgers University.

Serum biochemical analysis, hepatic lipid analysis, and glucose tolerance test

A panel of serum markers for assessing liver injury was measured, including concentrations of total cholesterol, triglycerides, and BAs, aspartate aminotransferase, alanine aminotransferase (ALT), and alkaline phosphatase enzymatic activities using commercially available kits (Pointe Scientific Inc). Frozen livers (100 mg) were used for lipid extraction with the previously reported method.^[24] The glucose tolerance test was conducted as previously reported by us.^[24,25]

Histological analysis

Fresh liver tissues were fixed overnight in 10% neutral buffered formalin. Hematoxylin and eosin staining was performed using a commonly used protocol. Collagen staining was performed using Masson's trichrome stain kit from Thermo Fisher Scientific (cat #87019). Histology was assessed by a pathologist with representative images captured by the Olympus VS120 slide scanning system shown in the figures.

Multiplex immunoassay analysis

Metabolic biomarkers in mouse serum were analyzed by MILLIPLEX metabolism multiplex assay (mouse metabolic hormone panel, MMHMAG044K, Millipore Sigma) through the Bio-Plex 200 system (Bio-Rad). Ten microliters of undiluted serum were used and all samples were run in duplicates. Serum levels of leptin and resistin are presented in this study.

Serum BA profiling

Serum BA from each individual mouse was extracted and 25 BA species were analyzed using the established protocol by the Rutgers Chemical Analysis Core

Facility.^[26,27] Quantitative profiling was performed using an Ultra Performance Liquid Chromatography/Electrospray/Ion Trap Mass Spectrometer (UPLC/ESI/ITMS, Thermo Fisher Scientific). Bile acid profiling is presented in ng/mL as mean \pm SD.

Gene expression

Total RNA was extracted from frozen liver, ileum, and brown adipose tissue using the TRIzol reagent (Thermo Fisher Scientific) and reverse transcription was performed to attain cDNA. Relative gene expression was determined by RT q-PCR by SYBR green chemistry using the ViiA7 Real-Time PCR machine (Life Technologies). All Ct values were converted to delta-delta Ct values and were normalized to β -actin mRNA levels. Primer sequences for mouse and human genes can be found in Supplemental Table S1, <http://links.lww.com/HC9/A890>.

Statistical analysis

Data are represented as mean \pm SD (n = 3–8/group). Outliers were removed using ROUT (Q = 2%). Comparisons of genotype within the same time point were performed using an unpaired *t* test followed by a 2-stage linear step-up procedure of Benjamini, Krieger, and Yekutieli. Comparison of groups to preop within a genotype was performed using 1-way ANOVA followed by Dunnett's multicomparison test with a single pooled variance. Human data comparison of groups was performed using one-way ANOVA. Spearman correlation with the Bonferroni correction method was employed to compare human samples. The results of statistical analysis were considered significant with *p* values < 0.05. Significance is denoted by a # or \$ for *t* test or 1-way ANOVA, respectively.

RESULTS

Hepatic gene expression in obese patients

The initial analysis of clinical data from obese patients revealed that despite their high average

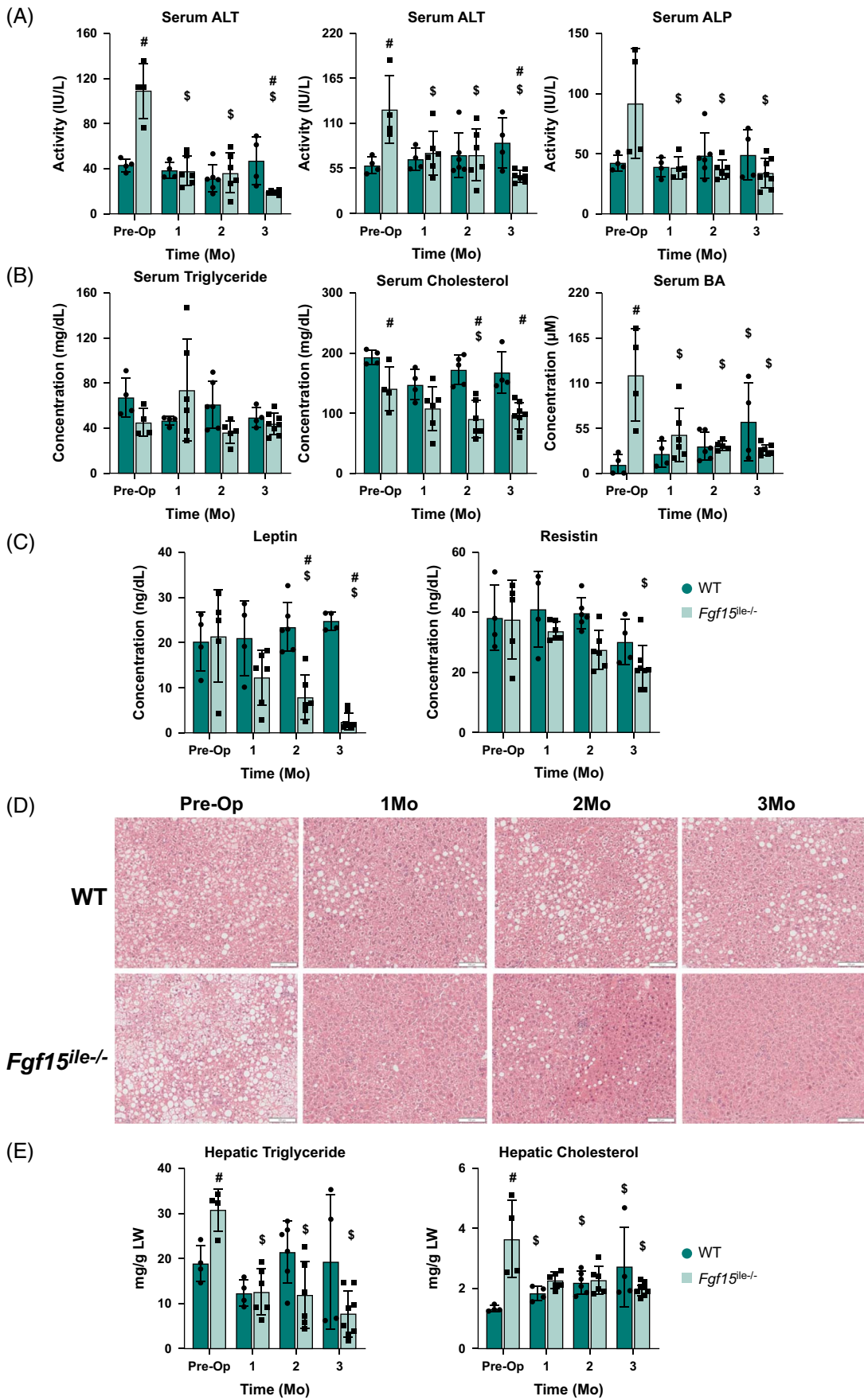


FIGURE 3 Effects of *Fgf15* deficiency on liver injury indexes and energy metabolism in the serum and pathology. (A) Serum ALT, AST, and ALP activity levels. (B) Serum triglycerides, cholesterol, and BA levels; (C) Serum leptin and resistin levels in WT and *Fgf15*^{ile-/-} mice at preop, 1, 2, and 3 months postop. (D) Liver HE staining and (E) hepatic triglyceride and total cholesterol levels in WT and *Fgf15*^{ile-/-} mice in the preop state, 1, 2, and 3-month HFD-fed mice following SGx (n = 4, 4, 6, 4 for WT, respectively; n = 5, 6, 6, 8 for *Fgf15*^{ile-/-}, respectively). Representative liver H&E stains at $\times 100$ magnification. \$ is for statistical significance ($p < 0.05$) within the same genotype compared to preop control. # is for statistical significance ($p < 0.05$) within the same time point. Abbreviations: ALP, alkaline phosphatase; ALT, alanine aminotransferase; AST, aspartate aminotransferase; BA, bile acid; H&E, hematoxylin and eosin; WT, wild type.

body mass index of 42.4, there was no substantial elevation observed in serum levels of total cholesterol, triglycerides, or liver functional indexes (ALT, aspartate aminotransferase, and alkaline phosphatase) (data not shown). Nevertheless, examination of hepatic gene expression exhibited a significant increase in mRNA levels of genes related to inflammation (*TNFA*, *IL1B*, and *LCN2*) and fibrosis (*COL1A1*), but exhibited only an upward trend for genes of *TIMP1* and *ACTA2* (Figure 1A). Moreover, there was a decrease in mRNA levels of *CYP7A1*, along with an increase in *FGF19*, *BSEP*, *SHP*, and *OSTb* mRNA levels, indicating potential hepatic cholestasis. While the mRNA levels of *CD36* were diminished in obese patients, minimal alterations were observed in the mRNA levels of *FXR*, *PPARa*, and *HNF4a*. Further scrutiny of the association between clinical data and hepatic gene expression revealed a positive correlation among *FGF19*, *OSTb*, and inflammation-associated genes, suggesting that disrupted BA homeostasis in obese patients might be interconnected with heightened inflammation (Figure 1B).

Effects of *Fgf15* deficiency on body weight (BW) changes after SGx in mice

One month following either sham or SGx, both WT and *Fgf15*^{ile-/-} mice showed a small drop in BW presumably due to the effects of the surgery. At both 2 and 3 months after SGx, WT mice showed a small reduction in BW compared to the sham group, but the *Fgf15*^{ile-/-} mice presented a much larger BW reduction compared to the sham group (Figure 2B). Therefore, the *Fgf15*^{ile-/-} mice reduced BW more than the WT mice did following SGx (Figure 2B). The reduction of WAT weight suggested that the greater BW decrease in the *Fgf15*^{ile-/-} mice may be due to WAT loss (Figure 2B). The *Fgf15*^{ile-/-} mice were more insulin sensitive suggested by the glucose tolerance test (Figure 2C). In general, the LW/BW ratio maintained at similar levels regardless of the differences in genotype, surgery, or HFD feeding. In addition, under sham operation, most comparisons between WT and *Fgf15*^{ile-/-} mice resulted in similar changes. Therefore, for succinct data presentation, Figures 3–7 will focus on the findings in WT and *Fgf15*^{ile-/-} mice following SGx.

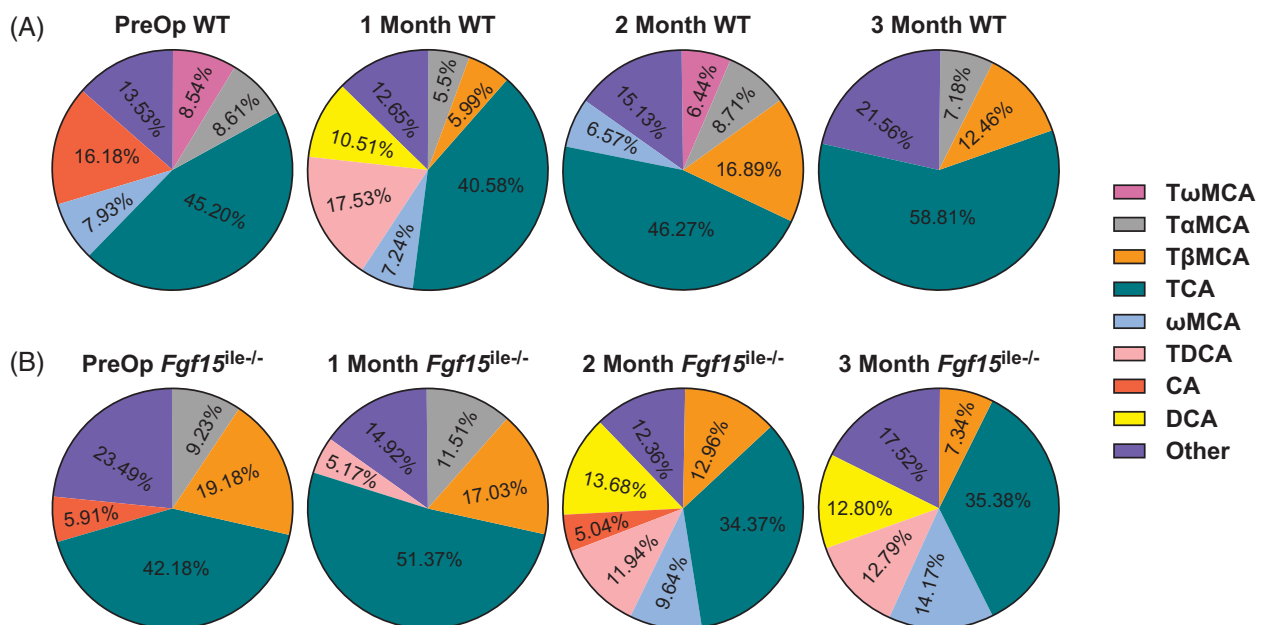


FIGURE 4 SGx altered serum BA composition in both (A) WT and (B) *Fgf15*^{ile-/-} mice. BA composition was determined by HPLC/MS in both WT and *Fgf15*^{ile-/-} mice at preop state, and 1, 2, and 3 months following SGx (n = 4, 4, 6, 4 for WT, respectively; n = 5, 6, 6, 8 for *Fgf15*^{ile-/-}, respectively). Abbreviations: BA, bile acid; SGx, vertical sleeve gastrectomy; WT, wild type.

TABLE 1 Bile acid concentration (ng/mL) in serum of mice with SGx

	Preop WT	Preop <i>Fgf15</i> ^{le-/-}	1 mo WT	1 mo <i>Fgf15</i> ^{le-/-}	2 mo WT	2 mo <i>Fgf15</i> ^{le-/-}	3 mo WT	3 mo <i>Fgf15</i> ^{le-/-}
Total TMCA	266.5 ± 172.0	36,095.2 ± 41,665.3	1243.9 ± 1287.9	15,250.3 ± 28,496.8	4635.1 ± 7603.1	6442.9 ± 9391.5	17,616.7 ± 14,506.0	3560.0 ± 3722.8 ^{a,b}
TωMCA	109.4 ± 101.4	3108.8 ± 3410.2	324.6 ± 235.0	246.3 ± 208.6	931.7 ± 1395.9	357.3 ± 226.5	2450.8 ± 1665.2 ^a	838.7 ± 757.0 ^b
TαMCA	110.4 ± 29.6	10717.7 ± 12213.5	440.3 ± 563.9	6051.4 ± 11511.5	1260.0 ± 1806.7	1410.6 ± 1320.0	5541.7 ± 4122.5 ^a	962.9 ± 733.7 ^{a,b}
TβMCA	46.7 ± 44.1	22,268.7 ± 26130.4	479.1 ± 529.3	8952.7 ± 17117.6	2443.9 ± 4431.2	4675.1 ± 8186.1	9624.2 ± 9821.3	1758.4 ± 2341.0 ^{a,b}
TUDCA	7.9 ± 12.7	2661.9 ± 2903.7	84.6 ± 136.5	858.4 ± 1483.0	210.3 ± 300.1	276.4 ± 307.0	1694.8 ± 1090.6	221.9 ± 167.4 ^{a,b}
THDCA	19.0 ± 10.4	149.5 ± 216.2	111.3 ± 134.2	161.4 ± 144.0	143.3 ± 182.3	253.9 ± 75.0	563.2 ± 327.8 ^a	232.8 ± 149.3 ^b
TCA	579.1 ± 211.4	48,968.9 ± 47,282.6	3246.6 ± 4582.3	26,999.9 ± 37,086.9	6694.0 ± 7569.7	12,395.2 ± 12,117.1	45,417.3 ± 31,967.6 ^a	8472.4 ± 5894.4 ^{a,b}
ωMCA	101.7 ± 86.6	4404.3 ± 4637.1	579.4 ± 515.3	1314.8 ± 1436.9	950.0 ± 1287.5	3478.3 ± 2166.3 ^b	3251.0 ± 2042.8 ^a	3392.0 ± 2549.7
αMCA	5.9 ± 11.8	761.5 ± 839.4	29.0 ± 39.6	153.9 ± 123.1	99.9 ± 170.7	285.8 ± 252.1	293.2 ± 160.5 ^a	134.2 ± 68.6 ^{a,b}
βMCA	61.0 ± 48.4	2785.6 ± 3530.3	105.8 ± 109.3	461.6 ± 435.7	156.9 ± 227.4	945.5 ± 1109.6	398.7 ± 388.7	461.8 ± 386.7
GCA	ND	120.9 ± 161.9	ND	28.20 ± 69.07	ND	ND	ND	ND
TCDCA	32.3 ± 5.6	4963.9 ± 5330.1	171.1 ± 247.1	2174.9 ± 3769.7	314.1 ± 292.1	593.3 ± 653.5	1929.8 ± 1385.8	518.6 ± 480.1 ^{a,b}
TDCA	0.5 ± 1.1	3045.4 ± 1786.7 ^b	1402.4 ± 2548.4	2714.6 ± 268.8	288.6 ± 374.6	4305.8 ± 2124.1 ^b	2278.6 ± 1193.9	3062.3 ± 1476.1
UDCA	ND	125.0 ± 145.2	14.0 ± 27.9	15.4 ± 27.0	7.9 ± 19.4	91.1 ± 106.4	27.3 ± 38.4	44.9 ± 45.5
CA	207.4 ± 259.7	6855.1 ± 7253.3	151.0 ± 302.0	338.0 ± 251.0	652.9 ± 1599.2	1819.4 ± 2470.6	1028.8 ± 1194.3	586.4 ± 567.8 ^a
HDCA	ND	153.7 ± 177.6	20.3 ± 40.6	72.3 ± 54.2	15.9 ± 39.0	244.3 ± 175.2 ^b	130.9 ± 106.1	192.4 ± 148.5
DCA	ND	4993.4 ± 3854.9 ^b	840.7 ± 1657.0	2013.9 ± 1004.2	299.1 ± 609.1	4935.6 ± 3027.2 ^b	2603.2 ± 2459.9	3064.1 ± 1396.6
Total	1281.3 ± 520.6	116,084.3 ± 115,390.6	8000.1 ± 11,584.8	52,557.6 ± 73,192.0	14,467.9 ± 19,927.4	36,067.4 ± 29,130.3	77,233.3 ± 55,744.9	23,943.9 ± 14,940.7 ^{a,b}

Note: Average concentrations of 17 bile acid species shown in ng/mL as part of profiling in both WT and *Fgf15*^{le-/-} mice at preop state, 1-, 2-, 3-month HFD-fed mice following SGx (n = 4, 4, 6, 4 for WT, respectively; n = 5, 6, 6, 8 for *Fgf15*^{le-/-}, respectively).

ND denotes not determined where concentration is below the limit of detection.

^aStatistical significance ($p < 0.05$) within the same genotype compared to preop control.

^bStatistical significance ($p < 0.05$) within the same time point.

Abbreviations: αMCA, α-Muricholic acid; βMCA, β-Muricholic acid; ωMCA, ω-Muricholic acid; CA, cholic acid; DCA, deoxycholic acid; GCA, glycocholic acid; HDCA, hyodeoxycholic acid; TCA, taurocholic acid; TCDCA, taurochenodeoxycholic acid; TDCA, taurodeoxycholic acid; THDCA, taurohyodeoxycholic acid; TMCA, taumuricholic acid; TUDCA, tauroursodeoxycholic acid; TαMCA, α-Taumuricholic acid; TβMCA, β-Taumuricholic acid; TωMCA, ω-Taumuricholic acid; UDCA, ursodeoxycholic acid.

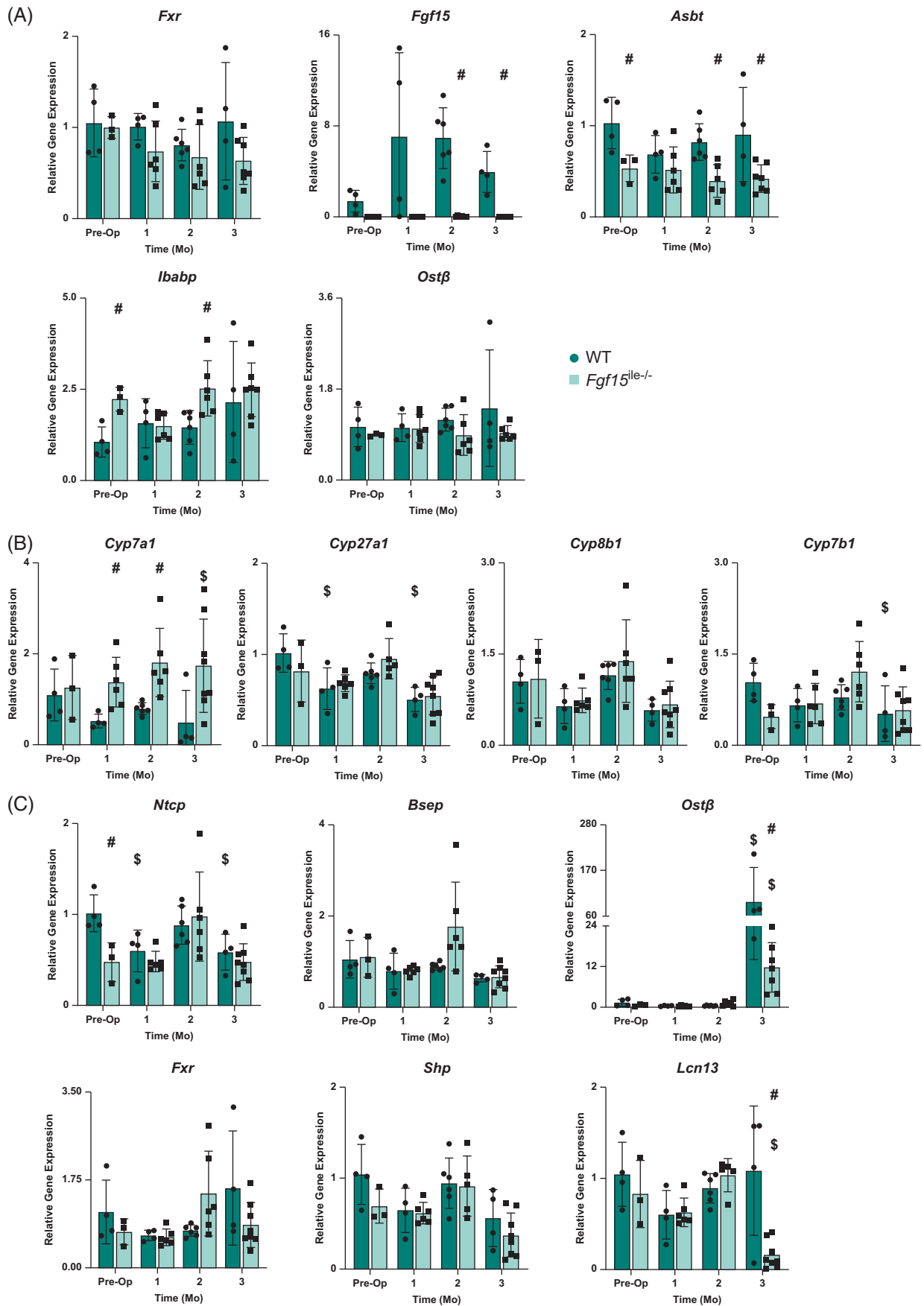


FIGURE 5 Effects of *Fgf15* deficiency on BA-related gene expression in the intestine and liver with SGx. (A) Relative mRNA levels of ileal genes associated with BA transport and regulation; (B) relative mRNA levels of BA synthesis genes in the liver; (C) relative mRNA levels of liver genes associated with BA transport and regulation in both WT and *Fgf15*^{ile-/-} mice at preop state, 1, 2, and 3-month HFD-fed mice following SGx. (n = 4, 4, 4 for WT, respectively; n = 5, 6, 6, 8 for *Fgf15*^{ile-/-}, respectively). \$ is for statistical significance ($p < 0.05$) within the same genotype compared to preop control. # is for statistical significance ($p < 0.05$) within the same time point. Abbreviations: BA, bile acid; SGx, vertical sleeve gastrectomy; WT, wild-type.

Effects of *Fgf15* deficiency on the progression of MASLD following SGx

Baseline preop serum activities of ALT, aspartate aminotransferase, and alkaline phosphatase were greater in *Fgf15*^{ile-/-} mice compared to WT, 2.5-, 2-, and 2-fold, respectively (Figure 3A). Post-SGx WT mice experienced slightly increased levels of these enzyme activities as the duration of HFD feeding continued by 3 months. However, all liver enzyme activities in *Fgf15*^{ile-/-} mice were reduced by SGx from 1 to 3 months after surgery (Figure 3A). The serum levels of triglycerides showed no difference between genotypes or by SGx (Figure 3B). Consistent with our previous studies,^[25] the serum total cholesterol levels were reduced after *Fgf15* deletion (preop) and continuously reduced in *Fgf15*^{ile-/-} mice after SGx at 1–3 months after surgery (Figure 3B). Consistent with a previous report,^[5] SGx resulted in higher serum total BA levels in WT mice (Figure 3B), but with *Fgf15* deficiency, the elevation of BAs was reduced by SGx (Figure 3B). The serum leptin and resistin levels showed similar trends of changes with ALT, total cholesterol, and total BAs (Figure 3C). Histologically, the 3-month HFD feeding resulted in classical features of liver macrovascular steatosis and SGx only slightly reduced steatosis in WT mice, because these mice continued to be fed HFD (Figure 3D). In contrast, the *Fgf15*^{ile-/-} mice showed marked improvement in hepatic steatosis, consistent with liver enzyme activity reduction by SGx (Figure 3D). Interestingly, slight inflammation was observed in the *Fgf15*^{ile-/-} group at 3 months after SGx, revealed by scattered foci of inflammation from the hematoxylin and eosin staining (Figure 3D). Hepatic triglyceride and total cholesterol levels further confirmed that lipid accumulation was continuously decreased in *Fgf15*^{ile-/-} after SGx, while triglyceride levels in WT mice decreased at 1 month after SGx, but returned to preop levels at 2–3 months after surgery (Figure 3E).

Effects of *Fgf15* deficiency on BA homeostasis after SGx

Taurine-conjugated cholic acid (TCA) is the most prominent BA species in the serum of both WT and *Fgf15*^{ile-/-} mice. In preop WT mice (Figure 4A), TCA made up about 45% of the total serum BAs and, in *Fgf15*^{ile-/-} mice, 42% (Figure 4B). TCA level increased in WT mice after SGx following 2- and 3-month HFD

feeding, making up 59% of the total serum BA pool (Figure 4A). Conversely, TCA levels decreased in *Fgf15*^{ile-/-} mice after SGx and following 1, 2, and 3 months of HFD feeding (Figure 4B). Unconjugated or taurine-conjugated DCA (TDCA) was unmeasurable in the serum of preop WT mice and was increased at 1, but not 2 and 3 months following SGx. In addition, there was an increase in taurine-conjugated muricholic acids in WT mice following SGx (Figure 4A). However, in *Fgf15*^{ile-/-} mice, SGx led to a reduction in MCAs, but an increase in DCA and TDCA across all time points (Figure 4B). Overall, the percent composition of serum BAs differs between WT and *Fgf15*^{ile-/-} mice and was differentially affected after SGx. Total serum BA levels were progressively increased in WT after SGx but stayed similarly in *Fgf15*^{ile-/-} mice after SGx compared to groups of preop. The exact concentration of the BA species is listed in Table 1.

Effects of *Fgf15* deficiency on expression of BA-related genes after SGx

FGF15 is critical for the suppression of BA synthesis and BAs are crucial in maintaining lipid homeostasis.^[14,15,25] Therefore, we examined the relative expression of genes involved in BA regulation and synthesis in the intestine and liver. In the intestine, *Fxr* expression in both WT and *Fgf15*^{ile-/-} mice showed no significance at preop and 1, 2, 3 months after SGx (Figure 5A). Following gene deletion, the *Fgf15*^{ile-/-} mice expressed very low, near undetectable mRNA levels of *Fgf15* with the WT mice having an increase at the 1- and 2-month postop period in response to SGx (Figure 5A). The expression of other genes involved in BA homeostasis was measured including apical sodium-dependent bile acid transporter (*Asbt*), ileal bile acid-binding protein (*Ibabp*), and organic solute transporter beta (*Ostβ*). *Asbt* expression remained consistent with preop levels with a slight decrease in expression at 1-month postop in WT mice and significantly increased expression compared to *Fgf15*^{ile-/-} mice counterparts preop, 2, and 3 months postop (Figure 5A). Unlike *Fxr* and *Asbt*, *Ibabp* expression increased following SGx with expression slightly decreased or equal to *Fgf15*^{ile-/-} counterparts. *Ibabp* expression in *Fgf15*^{ile-/-} mice was significantly increased at preop and 2 months compared to WT. In WT, *Ostβ* expression increased slightly following

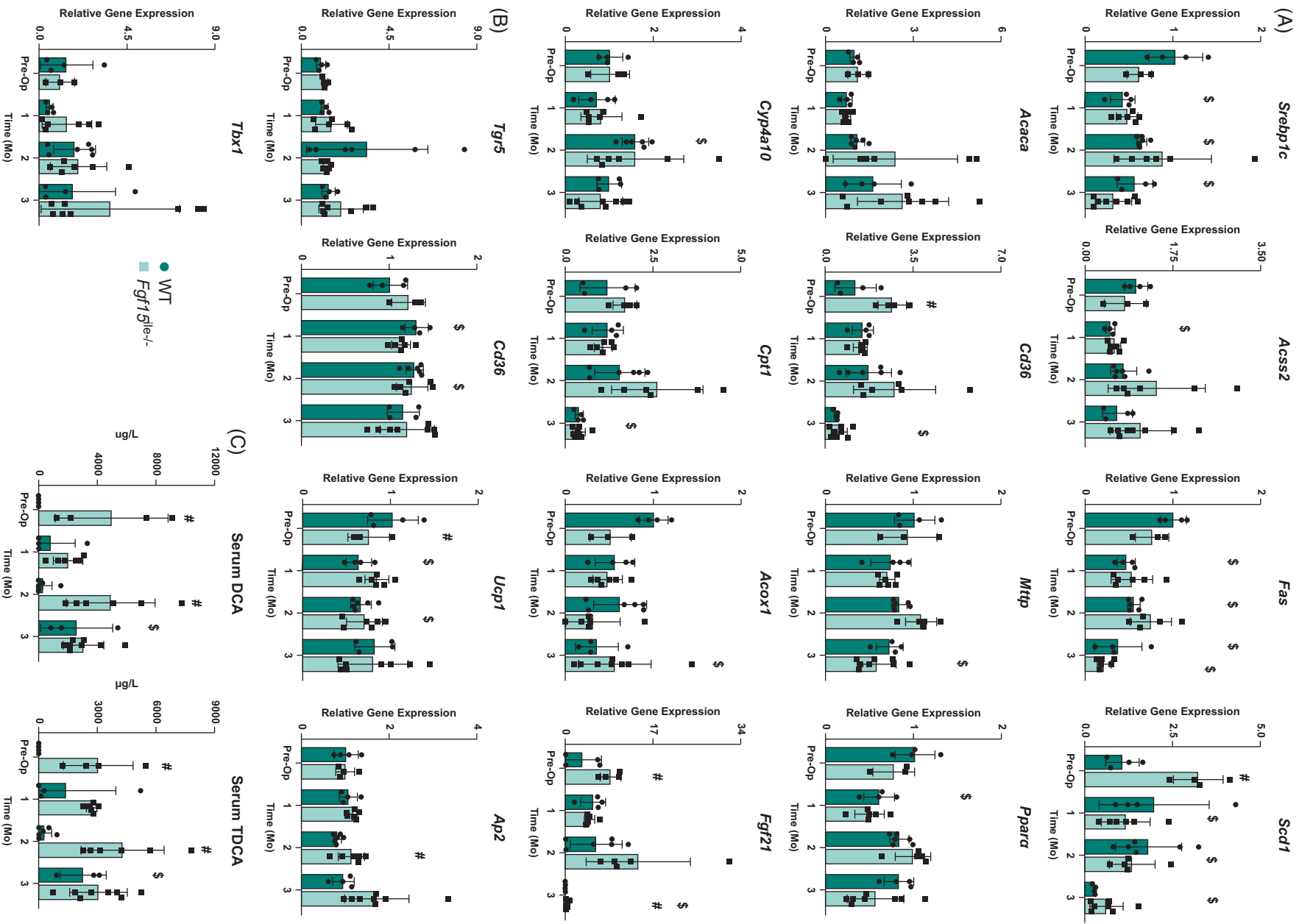


FIGURE 6 Effects of *Fgf15* deficiency on lipid-related gene expression in liver and BAT with SGx. (A) Relative mRNA levels of genes associated with lipid homeostasis; (B) relative mRNA levels of genes in BAT associated with adiposity and thermogenesis; (C) DCA and TDCA levels in the serum in both WT and *Fgf15*^{le-/-} mice at preop state, 1, 2, and 3-month HFD-fed mice following SGx (n = 4, 4, 6, 4 for WT, respectively; n = 5, 6, 6, 8 for *Fgf15*^{le-/-}, respectively). \$ is for statistical significance ($p < 0.05$) within the same genotype compared to preop control. # is for statistical significance ($p < 0.05$) within the same time point. Abbreviations: DCA, deoxycholic acid; HFD, high-fat diet; SGx, vertical sleeve gastrectomy; TDCA, taurine-conjugated DCA; WT, wild type.

surgery. On the other hand, *Ostβ* expression in *Fgf15*^{le-/-} mice remained consistent.

In the liver, the mRNA levels of genes involved in BA synthesis (*Cyp7a1*, *Cyp8b1*, *Cyp27a1*, and *Cyp7b1*) (Figure 5B) and transport (*Ntcp*, *Bsep*, and *Ostb*), as well as in BA regulation (*Fxr*, *Shp*, and *Lcn13*) (Figure 5C) were determined. In general, there was a small degree of reduction of mRNA levels of *Ntcp*, *Fxr*, and *Cyp7b1* in *Fgf15*^{le-/-} mice. However, little changed in the expression of these genes following SGx, except for *Cyp7a1*, which was reduced in WT mice and increased in *Fgf15*^{le-/-} mice, opposite with serum total BA changes. Furthermore, an FXR liver target gene that is specific to male mice, *Lcn13*, was markedly reduced in *Fgf15*^{le-/-} mice at 3 months after SGx. This is associated with a marked induction of *Ostβ* in WT mice at 3 months following SGx, with less induction in *Fgf15*^{le-/-} mice. This huge induction in *Ostβ* was not associated with cholestasis nor FXR activity, because signs of cholestasis or induction of other FXR target genes (*Shp*, *Bsep*, or *Lcn13*) were not seen.

Expression of genes involved in lipid homeostasis in the liver

The expression of genes involved in lipid synthesis (*Srebp1c*, *Acss2*, *Fas*, *Scd1*, and *Acaca*), fatty acid uptake (*Cd36*), triglyceride transfer (*Mttp*), beta-oxidation (*Ppara*, *Cyp4a10*), and energy regulation (*Cpt1* and *Fgf21*) were measured (Figure 6A). Before surgery (preop), compared with WT mice, the *Fgf15*^{le-/-} mice showed lower mRNA levels of *Srebp1c* and *Acox1*, higher levels of *Cd36*, *Scd1*, *Cpt1*, and *Fgf21*, and unaltered levels of *Mttp*, *Acss2*, consistent to increased BA levels and increased lipid absorption, which may lower the degree of hepatic de novo fatty acid synthesis. However, following SGx, there were fewer differences that may account for the decrease in hepatic lipid levels in *Fgf15*^{le-/-} mice.

Expression of genes involved in energy homeostasis in brown adipose tissue

Because the changes in expression of the liver lipid gene panel showed that reduction in liver lipid accumulation may not be due to reduced hepatic lipid synthesis, at least at the transcription level, and in light of the

increase in levels of TGR5 ligands, TDCA and DCA, in *Fgf15*^{le-/-} mice following SGx, the expression of genes in energy metabolism in brown adipose tissues was determined to see if increased TGR5 activity may contribute to the increased BW loss in *Fgf15*^{le-/-} mice (Figure 6B). The results showed that, in general, there was little difference between WT and *Fgf15*^{le-/-} mice for the expression of genes involved in lipid accumulation in adipose tissues regardless of surgery. However, the expression of *Tbx1*, which is involved in thermogenesis, and a target gene of TGR5 was induced by SGx in both strains of mice, with a higher degree in the *Fgf15*^{le-/-} mice, which were positively correlated with the serum DCA and TDCA levels (Figure 6C).

Expression of hepatic genes involved in inflammation and fibrosis

The expression of genes involved in inflammation (*Il-6*, *Tnfa*, *Cd14*, and *Tlr4*) was determined (Figure 7A). *Il-6* expression was significantly increased in both WT and *Fgf15*^{le-/-} mice 1- and 2-month following SGx compared to preop. This is followed by a large decrease at 3 months in both genotypes back to approximately preop levels. There was slightly increased expression in *Fgf15*^{le-/-} mice compared to WT postop which differed from preop where *Il-6* expression was higher in WT. *Tnfa* and *Cd14* expression followed a similar trend of *Il-6*. *Lcn2* mRNA levels had an overall increasing trend in *Fgf15*^{le-/-} mice. In WT mice, *Lcn2* expression increased at 1 month after surgery but decreased to preop levels at 2 months and continued to decrease to almost no expression at 3 months. The expression of genes involved in fibrosis was also determined (Figure 7B), and the results showed that Collagen 1A1 (*Col1a1*) expression in WT mice fluctuated at 1- and 2-month postop with a significant decrease at 1 month compared to preop, followed by a significant decrease at 3 months where there was virtually no expression. Compared to WT, *Fgf15*^{le-/-} mice showed a slight decrease at 1-month postop but an overall increasing trend with an increase from 1 to 3 months. The mRNA levels of smooth muscle alpha-actin (α SMA, *Acta2*) were similar between WT and *Fgf15*^{le-/-} mice with a marked reduction at 3 months in both groups. The mRNA levels of *Tgfb1* (TGF β) were markedly increased in *Fgf15*^{le-/-} mice preop but the expression was

suppressed with SGx, resulting in similar levels between WT and *Fgf15*^{ile-/-} mice. Figure 7C showed Trichrome staining for indication of fibrosis, and the results suggest there was no clear difference in the degree of fibrosis between WT and *Fgf15*^{ile-/-} mice following SGx, although as mentioned before, the degree of steatosis was markedly reduced in *Fgf15*^{ile-/-} mice.

Expression of genes involved in oxidative stress in the liver

Hmox1 expression in both WT and *Fgf15*^{ile-/-} mice was significantly decreased at 3 months with expression at 3 months after SGx significantly reduced compared to preop (Figure 7D). In addition, *Fgf15*^{ile-/-} was significantly increased 2 months following SGx.

CONCLUSIONS

Obesity poses a substantial global health care burden, and bariatric surgery remains the most effective treatment for morbid obesity.^[2,3] However, the underlying mechanism responsible for the beneficial effects of bariatric surgery remains unclear. Both circulating BAs and FGF19 levels were increased in patients with SGx^[4]; in addition, our hepatic gene expression results from human obese patients suggest increased cholestasis in the liver. BAs activate nuclear and membrane receptors to induce endocrine mediators, including FGF15/19, that aid in regulating energy expenditure.^[28,29] However, to what degree increased FGF15/19 mediates the beneficial effects of SGx remains obscure. In the current study, using HFD-induced obese mice with or without intestine-specific FGF15 deficiency, we have determined the roles that gut FGF15 plays in reducing obesity and improving MASLD following SGx.

Consistent with previously published reports,^[2,28] SGx led to increased total BA levels in WT mice. However, this increase does not appear to be mediating the improved energy homeostasis through the induction of FGF15, at least in our study. This is evident as our data showed that FGF15 deficiency enhanced body weight loss following SGx in mice, suggesting that FGF15-independent pathways are also involved in providing the beneficial effects of increase in BAs. This result is against our initial hypothesis because it is well known that increased FGF19 levels were shown in patients undergoing bariatric surgery and FGF15 promotes body weight loss^[8,17,18]; for example, a recent report showed that loss of FGF15 in the ileum did not lead to improved beneficial outcome but detrimental impacts due to BA toxicity.^[5] It is known that BAs also function as important signaling molecules that not only

activate nuclear receptors, including FXR but also membrane receptors, including TGR5, which regulates diverse physiological functions.^[19,21,29,30] The roles of FGF15 in mediating body weight loss and energy expenditure following SGx need to be further investigated.

It is well known that SGx alters many endocrine pathways.^[2,3] Previous studies have shown that serum levels of other gut hormones, including GLP1, have increased following SGx, which seems to be partially responsible for increased energy expenditure and body weight loss.^[20,21] Our study has demonstrated that FGF15-deficient mice had better metabolic outcomes after SGx, including more weight loss and less liver steatosis. These improvements are accompanied by changes in the BA profile. Following serum BA composition analysis, our study showed that serum concentrations of several secondary BAs, including DCA and TDCA, were increased. These BA species are known to be ligands of the membrane BA receptor, TGR5. Activation of TGR5 is known to increase thermogenesis and improve energy expenditure, for example, through the induction of GLP1 or an increase in thermogenesis.^[19,21,29,30] Even though we did not successfully detect circulation levels of GLP1 in the current study, changes in the mRNA levels of several TGR5 target genes in the brown adipose tissue suggest there may be an increase in TGR5 activity, revealed by induction of a TGR5 target gene, *Tbx1*. Ding et al^[28] have reported that TGR5 activation is involved in improved metabolic outcomes following bariatric surgery. Hepatic steatosis was drastically improved at our earliest time point of one month.

Furthermore, our study suggests that BAs and/or FGF15 pathways may interact with other endocrine pathways that are important for adiposity and insulin sensitivity. For instance, we observed a time-dependent reduction in the serum circulating levels of leptin and resistin in the *Fgf15*^{ile-/-} mice following SGx. The involvement of these pathways needs to be determined in the future to clarify how the alternations in these signaling pathways can play a role in improving metabolic outcomes. Furthermore, it will be interesting to determine whether increased BAs also play a role in reducing these hormones.

We have observed in several studies that there is a positive association between ALT activities and total cholesterol levels, but a negative association of total levels of serum BAs, with advanced MASH progression.^[24,25] Interestingly, hepatic gene expression for inflammatory genes does not seem to be associated with the severity of liver injury. For example, the expression of 2 inflammatory genes, *Il-6* and *Tnfa*, was markedly induced at 1- and 2-month after surgery in both WT and *Fgf15*^{ile-/-} mice, which may reflect the liver's response to major abdominal surgery, but not at 3 months. It will be insightful to obtain other

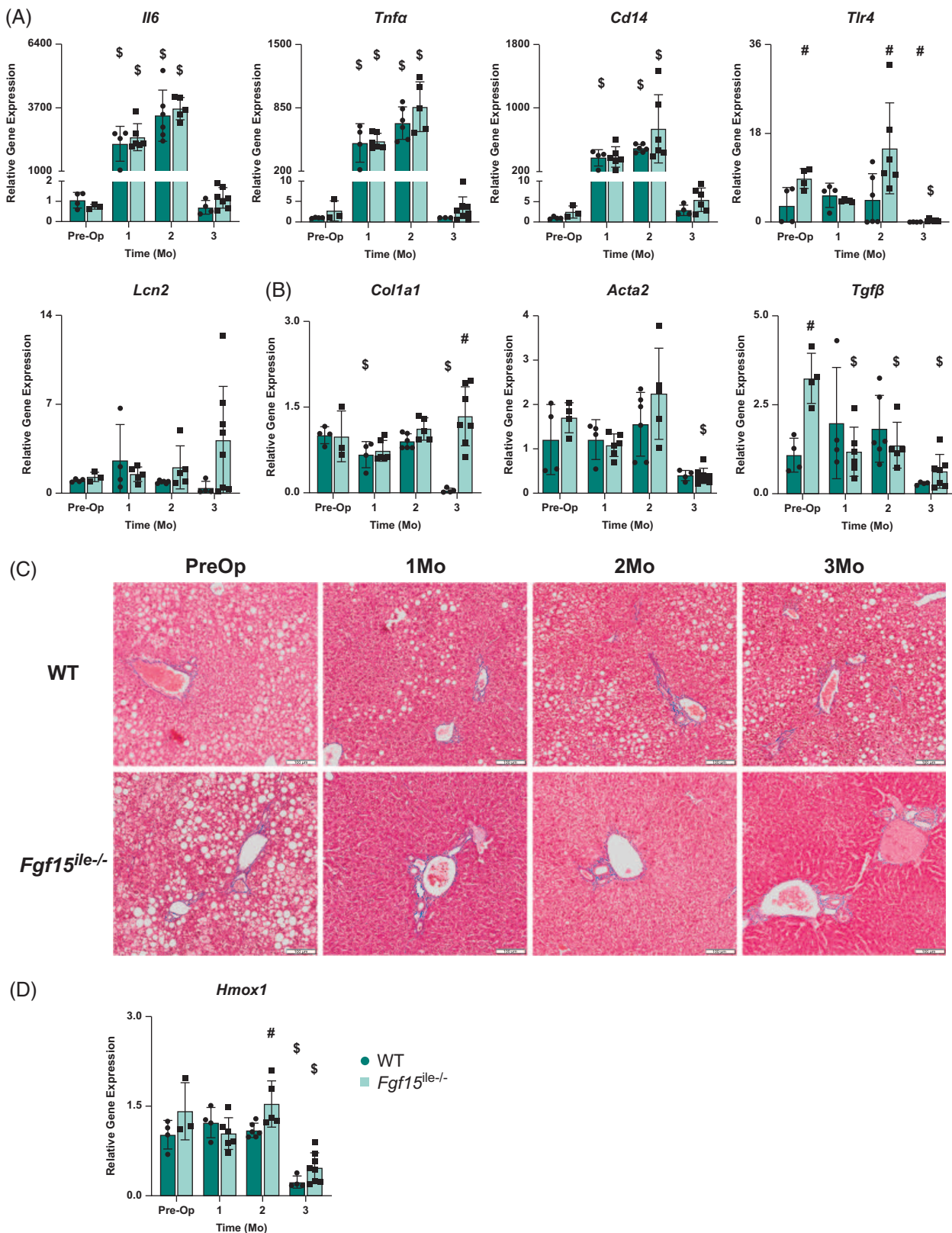


FIGURE 7 Effects of *Fgf15* deficiency on inflammation, fibrosis, and oxidative stress-related gene expression in the liver with SGx. (A) Relative mRNA levels of genes associated with inflammation; (B) relative mRNA levels of genes associated with fibrosis; (C) trichrome staining of the liver; (D) relative mRNA levels of gene *Hmox1* associated with oxidative stress in both WT and *Fgf15^{ile-/-}* mice at preop state, 1, 2, and 3-month HFD-fed mice following SGx (n = 4, 4, 6, 4 for WT, respectively; n = 5, 6, 6, 8 for *Fgf15^{ile-/-}*, respectively). \$ is for statistical significance ($p < 0.05$) within the same genotype compared to preop control. # is for statistical significance ($p < 0.05$) within the same time point. Abbreviations: HFD, high-fat diet; SGx, vertical sleeve gastrectomy; WT, wild type.

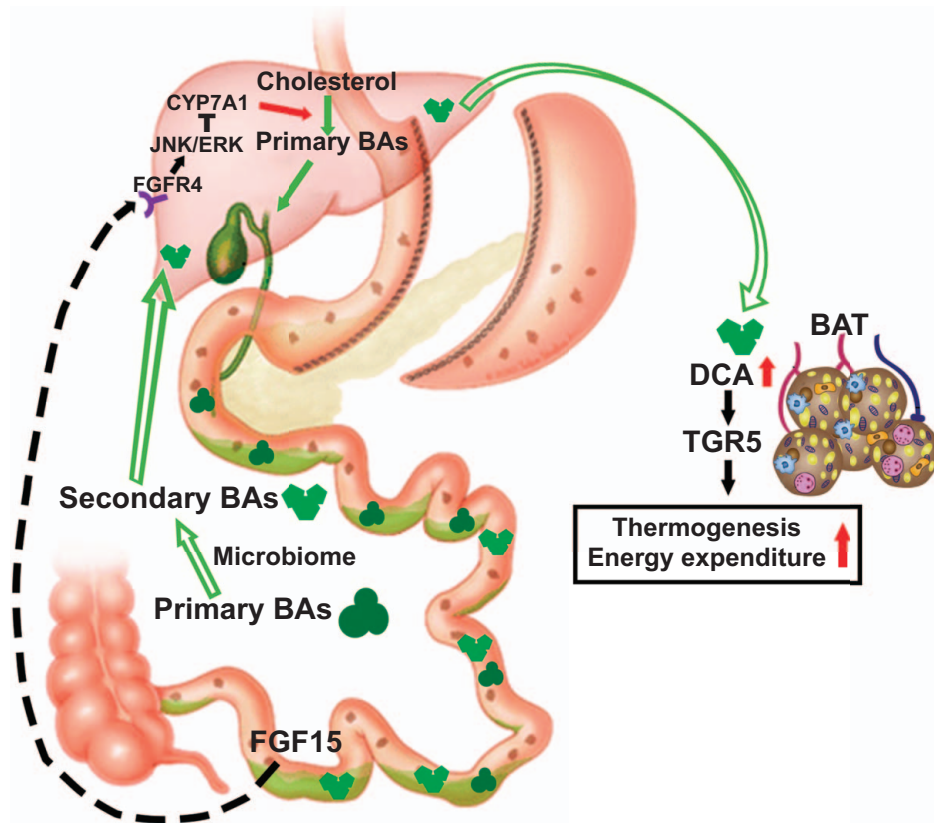


FIGURE 8 Proposed effects of the gut-specific deletion of *Fgf15* on energy expenditure in the brown adipocytes following SGx. Abbreviation: SGx, vertical sleeve gastrectomy.

inflammatory markers for chronic liver inflammation, and in our hands, the expression of *Lcn2* that encodes for an acute phase protein lipocalin 2 has been associated with steatotic liver inflammation.^[24,25,31]

In conclusion, following SGx, the gut-specific deletion of FGF15 leads to an increased BA pool in the body due to the decreased feedback inhibition of BA synthesis mediated by FGF15. Increased BAs in the intestine likely remodel the gut microbiota, and thus the conversion of secondary BAs from primary BAs. Increased systemic circulation of secondary BAs, such as DCA and TDCA, may have acted as endogenous TGR5 agonists to activate the TGR5 signaling in the brown adipocytes, which thereby improves insulin sensitivity, promotes adipose tissue browning, energy expenditure, and ultimately BW loss (Figure 8). This BA-dependent mechanism has been involved in the protection against diet-induced hepatic steatosis and fibrogenesis in FXR KO and *Fgf15*^{ile-/-} mice.^[25,31,32]

AUTHOR CONTRIBUTIONS

Monica D. Chow, Katherine Otersen, Andrew Wassef, Bo Kong, and Sowmya Yamarthy planned and performed the animal surgery. Daniel Rizzolo, III Yang, Brian Buckley, Alexander Lu, Naomi Crook, Matthew Lee, Judy Gao, Sareena Naganand, Mary F. Stofan,

Laura Armstrong, Justin Schumacher, Rulaiha Taylor, Zakiyah Henry, Veronia Basaly, Zhenning Yang, Min Zhang, and Mingxing Huang assisted with the data collection and data analysis. Leonid Kagan, Luigi Brunetti, Ragui Sadek, Yi-Horng Lee, and Grace L. Guo collected patient data and supervised the project. Yi-Horng Lee and Grace L. Guo conceived the original idea. Katherine Otersen, Andrew Wassef, Bo Kong, Sowmya Yamarthy, and Grace L. Guo wrote the paper with input from all authors. All authors made a significant contribution to the work and shared the responsibility. All authors have read and approved the final version for publication.

ACKNOWLEDGMENTS

Dr. Pamela Ohman-Strickland, the in-house statistician from Rutgers EOHSI, guided the statistical analysis. Angelica Hanna, the medical student from Touro College of Medicine, aided in data extraction and bioanalytics. Dr. Omar Gonzalez, general surgery resident from Rutgers Robert Wood Johnson Medical School, aided in human liver specimen collection. Drs. Michael Donaire, Lora Melman, Keith King, Heath Antione, Siddharth Kudav, Mrs. Lisa Siracusa, and physician assistants from Advanced Surgical & Bariatrics of NJ surgeons aided in human liver specimen collection.

FUNDING INFORMATION



This work was supported by the National Institutes of Health (Grants: T32ES007148, GM134258, ES029258, DK122725, R01GM135258, and R01GM124046), the Department of Veteran Affairs (BX002741), Rutgers University Center for Research, and Robert Wood Johnson Foundation.

CONFLICTS OF INTEREST

Justin Schumacher owns stock and is employed by Bristol Myers Squibb. Luigi Brunetti received grants from Merck and CSL Behring. The remaining authors have no conflicts to report.

ORCID

Katherine Otersen  <https://orcid.org/0000-0001-5921-110X>

Bo Kong  <https://orcid.org/0000-0002-8200-7817>
Sowmya Yamarthy  <https://orcid.org/0000-0002-2146-8396>

Daniel Rizzolo  <https://orcid.org/0000-0002-6145-989X>

Ill Yang  <https://orcid.org/0000-0002-5665-6012>

Brian Buckley  <https://orcid.org/0000-0001-7336-4321>

Alexander Lu  <https://orcid.org/0009-0000-5847-1233>

Mary F. Stofan  <https://orcid.org/0000-0002-0435-9809>

Laura Armstrong  <https://orcid.org/0000-0002-7351-0701>

Justin Schumacher  <https://orcid.org/0000-0002-9900-4989>

Rulaiha Taylor  <https://orcid.org/0000-0002-0561-3653>

Zakiyah Henry  <https://orcid.org/0000-0002-6272-8115>

Veronia Basaly  <https://orcid.org/0000-0002-1830-4809>

Zhenning Yang  <https://orcid.org/0000-0003-0989-5544>

Min Zhang  <https://orcid.org/0000-0003-2497-6748>

Mingxing Huang  <https://orcid.org/0000-0002-7884-8752>

Luigi Brunetti  <https://orcid.org/0000-0003-0565-6167>

Yi-Hong Lee  <https://orcid.org/0000-0003-2796-6983>

Grace L. Guo  <https://orcid.org/0000-0002-2666-0635>

REFERENCES

- Chow MD, Lee YH, Guo GL. The role of bile acids in nonalcoholic fatty liver disease and nonalcoholic steatohepatitis. *Mol Aspects Med.* 2017;56:34–44.
- Tu J, Wang Y, Jin L, Huang W. Bile acids, gut microbiota and metabolic surgery. *Front Endocrinol (Lausanne).* 2022;13:929530.
- Abbatini F, Rizzello M, Casella G, Alessandri G, Capoccia D, Leonetti F, et al. Long-term effects of laparoscopic sleeve gastrectomy, gastric bypass, and adjustable gastric banding on type 2 diabetes. *Surg Endosc.* 2010;24:1005–10.
- Nakatani H, Kasama K, Oshiro T, Watanabe M, Hirose H, Itoh H. Serum bile acid along with plasma incretins and serum high-molecular weight adiponectin levels are increased after bariatric surgery. *Metabolism.* 2009;58:1400–7.
- Myronovych A, Bhattacharjee J, Salazar-Gonzalez RM, Tan B, Mowery S, Ferguson D, et al. Assessment of the role of FGF15 in mediating the metabolic outcomes of murine Vertical Sleeve Gastrectomy (VSG). *Am J Physiol Gastrointest Liver Physiol.* 2020;319:G669–84.
- Wu Q, Zhang X, Zhong M, Han H, Liu S, Liu T, et al. Effects of bariatric surgery on serum bile acid composition and conjugation in a diabetic rat model. *Obes Surg.* 2016;26:2384–92.
- Guo GL, Lambert G, Negishi M, Ward JM, Brewer HB, Kliewer SA, et al. Complementary roles of farnesoid X receptor, pregnane X receptor, and constitutive androstane receptor in protection against bile acid toxicity. *J Biol Chem.* 2003;278:45062–71.
- Lalloyer F, Mogilenko DA, Verrijken A, Haas JT, Lamazière A, Kouach M, et al. Roux-en-Y gastric bypass induces hepatic transcriptomic signatures and plasma metabolite changes indicative of improved cholesterol homeostasis. *J Hepatol.* 2023;79:898–909.
- Henry Z, Meadows V, Guo GL. FXR and NASH: An avenue for tissue-specific regulation. *Hepatol Commun.* 2023;7:e0127.
- Meadows V, Yang Z, Basaly V, Guo GL. FXR friend-ChIPs in the enterohepatic system. *Semin Liver Dis.* 2023;43:267–78.
- Wang H, Chen J, Hollister K, Sowers LC, Forman BM. Endogenous bile acids are ligands for the nuclear receptor FXR/BAR. *Mol Cell.* 1999;3:543–53.
- Ryan KK, Tremaroli V, Clemmensen C, Kovatcheva-Datchary P, Myronovych A, Karns R, et al. FXR is a molecular target for the effects of vertical sleeve gastrectomy. *Nature.* 2014;509:183–8.
- Kim I, Ahn SH, Inagaki T, Choi M, Ito S, Guo GL, et al. Differential regulation of bile acid homeostasis by the farnesoid X receptor in liver and intestine. *J Lipid Res.* 2007;48:2664–72.
- Kong B, Wang L, Chiang JYL, Zhang Y, Klaassen CD, Guo GL. Mechanism of tissue-specific farnesoid X receptor in suppressing the expression of genes in bile-acid synthesis in mice. *Hepatology.* 2012;56:1034–43.
- Song KH, Li T, Owsley E, Strom S, Chiang JYL. Bile acids activate fibroblast growth factor 19 signaling in human hepatocytes to inhibit cholesterol 7 α -hydroxylase gene expression. *Hepatology.* 2009;49:297–305.
- Inagaki T, Choi M, Moschetta A, Peng L, Cummins CL, McDonald JG, et al. Fibroblast growth factor 15 functions as an enterohepatic signal to regulate bile acid homeostasis. *Cell Metab.* 2005;2:217–25.
- Marcelin G, Jo YH, Li X, Schwartz GJ, Zhang Y, Dun NJ, et al. Central action of FGF19 reduces hypothalamic AGRP/NPY neuron activity and improves glucose metabolism. *Mol Metab.* 2014;3:19–28.
- Kong B, Sun R, Huang M, Chow MD, Zhong XB, Xie W, et al. Fibroblast growth factor 15-dependent and bile acid-independent promotion of liver regeneration in mice. *Hepatology.* 2018;68:1961–76.
- Kawamata Y, Fujii R, Hosoya M, Harada M, Yoshida H, Miwa M, et al. A G protein-coupled receptor responsive to bile acids. *J Biol Chem.* 2003;278:9435–40.
- Chen JS, Chang LC, Wu CC, Yeung LK, Lin YF. Involvement of F-actin in chaperonin-containing t-complex 1 beta regulating mouse mesangial cell functions in a glucose-induction cell model. *Exp Diabetes Res.* 2011;2011:565647.
- Velazquez-Villegas LA, Perino A, Lemos V, Zietak M, Nomura M, Pols TWH, et al. TGR5 signalling promotes mitochondrial fission

- and beige remodelling of white adipose tissue. *Nat Commun.* 2018;9:245.
22. Bozadjieva-Kramer N, Shin JH, Shao Y, Gutierrez-Aguilar R, Li Z, Heppner KM, et al. Intestinal-derived FGF15 protects against deleterious effects of vertical sleeve gastrectomy in mice. *Nat Commun.* 2021;12:4768.
 23. Rizzolo D, Kong B, Piekos S, Chen L, Zhong X, Lu J, et al. Effects of overexpression of fibroblast growth factor 15/19 on hepatic drug metabolizing enzymes. *Drug Metab Dispos.* 2022; 50:468–77.
 24. Taylor R, Armstrong L, Bhattacharya A, Henry Z Brinker A, Buckley B, et al. Myclobutanil-mediated alteration of liver-gut FXR signaling in mice. *Toxicol Sci.* 2023;191: 387–99.
 25. Schumacher JD, Kong B, Pan Y, Zhan L, Sun R, Aa J, et al. The effect of fibroblast growth factor 15 deficiency on the development of high fat diet induced non-alcoholic steatohepatitis. *Toxicol Appl Pharmacol.* 2017;330:1–8.
 26. Zhan L, Yang I, Kong B, Shen J, Gorczyca L, Memon N, et al. Dysregulation of bile acid homeostasis in parenteral nutrition mouse model. *Am J Physiol Gastrointest Liver Physiol.* 2016; 310:G93–102.
 27. Rizzolo D, Buckley K, Kong B, Zhan L, Shen J, Stofan M, et al. Bile acid homeostasis in a cholesterol 7 α -hydroxylase and sterol 27-hydroxylase double knockout mouse model. *Hepatology.* 2019;70:389–402.
 28. Ding L, Sousa KM, Jin L, Dong B, Kim BW, Ramirez R, et al. Vertical sleeve gastrectomy activates GPBAR-1/TGR5 to sustain weight loss, improve fatty liver, and remit insulin resistance in mice. *Hepatology.* 2016;64:760–73.
 29. Pathak P, Liu H, Boehme S, Xie C, Krausz KW, Gonzalez F, et al. Farnesoid X receptor induces Takeda G-protein receptor 5 cross-talk to regulate bile acid synthesis and hepatic metabolism. *J Biol Chem.* 2017;292:11055–69.
 30. Chiang JYL, Ferrell JM. Bile acid receptors FXR and TGR5 signaling in fatty liver diseases and therapy. *Am J Physiol Gastrointest Liver Physiol.* 2020;318:G554–73.
 31. Schumacher JD, Kong B, Wu J, Rizzolo D, Armstrong LE, Chow MD, et al. Direct and indirect effects of fibroblast growth factor (FGF) 15 and FGF19 on liver fibrosis development. *Hepatology.* 2020;71:670–85.
 32. Zhang Y, Ge X, Heemstra LA, Chen WD, Xu J, Smith JL, et al. Loss of FXR protects against diet-induced obesity and accelerates liver carcinogenesis in ob/ob mice. *Mol Endocrinol.* 2012; 26:272–80.

How to cite this article: Chow MD, Otersen K, Wassef A, Kong B, Yamarthy S, Rizzolo D, et al. Effects of intestine-specific deletion of FGF15 on the development of fatty liver disease with vertical sleeve gastrectomy. *Hepatol Commun.* 2024;8: e0444. <https://doi.org/10.1097/HC9.0000000000000444>